Multifunctional Polymer Coatings for Cell Microarray Applications

ARTICLE *in* BIOMACROMOLECULES · APRIL 2009

Impact Factor: 5.75 · DOI: 10.1021/bm801417s · Source: PubMed

Article

Multifunctional Polymer Coatings for Cell Microarray Applications

Mahaveer D. Kurkuri, Chantelle Driever, Graham Johnson,
Gail McFarland, Helmut Thissen, and Nicolas H. Voelcker

Biomacromolecules, **Article ASAP** • DOI: 10.1021/bm801417s • Publication Date (Web): 30 March 2009

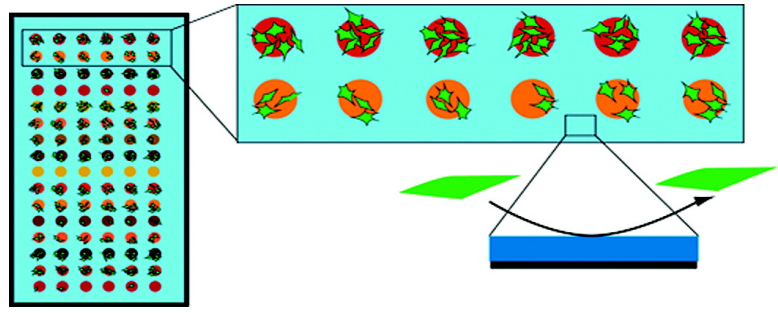

Multifunctional Polymer Coatings for Cell Microarray Applications

Mahaveer D. Kurkuri,[†] Chantelle Driever,[‡] Graham Johnson,[§] Gail McFarland,[§] Helmut Thissen,*[,‡,||] and Nicolas H. Voelcker*[,†,||]

School of Chemistry, Physics and Earth Sciences, Flinders University, GPO Box 2100, Bedford Park SA 5042, Australia, CSIRO Molecular and Health Technologies, Bayview Avenue, Clayton VIC 3168, Australia, CSIRO Molecular and Health Technologies, Riverside Corporate Park, 11 Julius Avenue, North Ryde NSW 2113, Australia, and CSIRO Food Futures Flagship, Riverside Corporate Park, 5 Julius Avenue, North Ryde NSW 2113, Australia

Received December 7, 2008; Revised Manuscript Received February 16, 2009

Biocompatible coatings with suitable chemistries for the immobilization of biomolecules are increasingly in demand, as they can be applied in a wide range of biomedical applications. In particular, multifunctional polymer coatings displaying reactive functional groups for the immobilization of specific biological factors that can influence the cellular response while at the same time exhibiting low nonspecific protein adsorption and cell attachment properties have the potential to significantly advance the fields of biomaterials and regenerative medicine. In this study, multifunctional polymer surface chemistries were developed for a cell microarray application with the aim of screening cellular interactions with surface immobilized factors. Coatings were prepared by the deposition of an allylamine plasma polymer pinning layer followed by the deposition of random copolymers of glycidyl methacrylate (GMA) and poly(ethylene glycol) methacrylate (PEGMA). Coatings were characterized by X-ray photoelectron spectroscopy (XPS), infrared spectroscopy, ellipsometry, and contact angle measurements. A variety of proteins as well as synthetic polymers were printed onto copolymer-coated slides using a high-precision contact microarrayer. Printing conditions were optimized for a fluorescently labeled model protein in regard to the temperature, humidity, pin geometry, concentration, and pH of the printing solution. Finally, the suitability of the surface chemistry for the evaluation of cellular responses to surface immobilized factors in a microarray format was demonstrated using HeLa cells.

Introduction

Microarrays allow the analysis of a large number of biomolecular interactions. Particularly, DNA and protein microarrays have been highly successful and have facilitated the screening of such interactions in a rapid, low-cost, and low-volume format.[1−6] In recent years, this highly successful format has been extended to the screening of cell−biomolecule and more generally to cell−material surface interactions. Here, the cell microarray format[7] allows the high throughput screening of cellular responses such as cell attachment, viability, morphology, and change in phenotype in response to signals displayed on the array surface. Cell microarrays can therefore contribute to the trajectory of innovation in a field that traditionally relies on low-throughput experimental setups, operating under conditions where large amounts of support material, biomolecules, cell culture media, and cells are required, contributing to high analysis costs.

Important design criteria for cell microarrays include the need for the prevention of cell attachment between areas that display different signals, the need for a sufficient surface area in which the signals are displayed (in order to be able to observe sufficient cell numbers for statistical evaluation) and the need for printing multiple areas with the same signal (in order to improve the confidence). Various techniques have been harnessed for the preparation of cell microarrays. They include self-assembled monolayers (SAMs) of alkanethioles on gold-coated glass plates, combined with patterning by a UV/masking technique,[3] the use of holey paraffin molds on coated glass slides,[8] excimer-patterning of PTFE foils in an NH_3 atmosphere,[9] and many more.

Recent reviews[10,11] have highlighted applications of cell microarrays such as the identification of populations of cells, the characterization of cell phenotypes and states, and the monitoring of cell function. Increasingly, cell microarrays are also used in drug discovery applications. Furthermore, the high-throughput cell microarray format has inspired the development of many other techniques based on this format such as transfected cell microarrays.[12,13]

Examples for cell−material interaction studies based on cell microarrays include studies by Anderson et al.,[14,15] where various polymers were printed to characterize human embryonic stem cell−material interactions. Furthermore, Mant et al.[16] microarrayed a range of polyurethanes to screen the interactions with bone marrow dendritic cells, Ito et al.[17] spotted photoreactive polymers and proteins for COS-7 cell attachment studies, and Flaim et al.[18] printed combinations of five extracellular matrix molecules on polyacrylamide gel-coated slides to probe cellular differentiation. Likewise, Soen et al. printed combinations of extracellular matrix proteins, but also included morphogens and other signaling proteins to investigate effects of

* Corresponding author. E-mail: nico.voelcker@flinders.edu.au; telephone: +61 8 8201 5338; fax: +61 8 8201 2905 (N.H.V.). E-mail: helmut.thissen@csiro.au; telephone: +61 3 9545 2191; fax: +61 3 9545 2446 (H.T.).

[†] Flinders University.

[‡] CSIRO Molecular and Health Technologies, Clayton.

[§] CSIRO Molecular and Health Technologies, North Ryde.

[||] CSIRO Food Futures Flagship.

10.1021/bm801417s CCC: $40.75

the surface-bound signals on proliferation and phenotype of primary neural precursor cells.[19]

Increasing attention has been devoted to the development of suitable material chemistry platforms that enable the immobilization of factors on the microarray surface. Here, the most commonly used base materials are transparent and include particularly glass and polymers such as polystyrene.[16−20] However, substrates such as gold, other metals, and silicon wafers have been used as well.[21−23] The deposition of biomolecules on these substrates is typically achieved through a coating representing a biomolecule-reactive layer, deposited by dip or spin coating,[16] surface grafting,[20,24] plasma treatment,[25] SAM formation,[3] and microfluidic[26] and microspotting[17] techniques. The key requirements for such coatings are manifold. First, these coatings must be stable and remain pinhole-free under the conditions used for microarray preparation and processing. Second, these coatings must enable the immobilization of biomolecules or synthetic factors that are arrayed onto the surface, and, third, these coatings must give a low cell attachment background on all areas of the substrate that are not covered by printed factors. Finally, it is imperative that these coatings do not interfere with the readout signal used to analyze the microarrays.

The presence of primary amines in many biomolecules of interest provide an adequate target for reactive functional groups displayed on the array surface. A variety of amine-reactive functional groups such as *N*-hydroxy succinimide esters, aldehydes, isocyanates, and epoxide groups are well established.[27] The reduction of nonspecific protein adsorption and subsequent cell attachment in the regions surrounding the microarrayed spots can be achieved by using solutions of surfactants such as Pluronic3 or proteins such as bovine serum albumin (BSA).[28] However, problems with desorption and high fluorescence background often limits the sensitivity of microarray platforms prepared in this way. An alternative passivation technique often used in biomedical applications is the grafting of poly(ethylene glycol) (PEG). High-density PEG coatings have been shown to reduce protein adsorption to levels that are at the limit of currently available analytical techniques and to completely prevent cell attachment.[29,30] PEG-based microarray coatings have already been described in the literature. For example, Kannan et al.[31] reported a lithography-based technique on glass slides to fabricate patterns of functional molecules surrounded by a PEG matrix for applications in protein microarrays.

In this study, we set out to prepare multifunctional coatings based on copolymers made from poly(ethylene glycol) methyl ether methacrylate (PEGMA). Protein printing conditions on the copolymer coatings were optimized. Finally, cell attachment results on arrays printed with a range of biological factors and synthetic polymers are presented to illustrate the suitability of these multifunctional coatings in cell microarray applications that satisfy the critical requirements for microarray coatings and avoid some of the issues of previous platforms. In particular, our approach is engineering-friendly and virtually independent of the underlying substrate. Furthermore, a chemical activation step for covalent attachment of biomolecules is not required.

Materials and Methods

Substrate Preparation. Precleaned microscope glass slides obtained from Biolab (USA) were further cleaned by sonication in surfactant solution (2% RBS (Pierce, USA), 2% ethanol, 96% MilliQ water) for 1 h and then washed with Milli-Q water. Slides were then placed into a 1 M NaOH solution for 5 min, washed thoroughly in Milli-Q water and dried using a spin dryer (Technical Video, LTD). P-type silicon wafers with an orientation of 1−0−0 and a resistivity of 10−20 Ω·cm were obtained from Silicon Quest International (USA) and cleaned in the same way as the glass slides.

Table 1. List of Coating Methods and Copolymer Compositions Used in This Study

coating method	copolymer ratio (PEGMA:GMA) (w:w)	code
dip coating	2:1	DC2:1
	1:1	DC1:1
	1:2	DC1:2
grafting	1:1	G1:1
spin coating	1:1	SC1:1

Plasma Polymerization. Plasma polymerization experiments were carried out in a custom-built reactor as described elsewhere.[32] Briefly, the cylindrical reactor chamber was defined by a height of 35 cm and a diameter of 17 cm. The lower and upper electrodes were both circular, with a diameter of 10.5 cm and separation of 16 cm. Samples were placed on the lower electrode. Allylamine (Aldrich, Australia, 98% purity) plasma polymer (ALAPP) coatings were deposited using a frequency of 200 kHz, a power of 20 W, an initial monomer pressure of 0.230 mbar and a treatment time of 25 s. This procedure resulted in a pinhole-free plasma polymer with a film thickness of approximately 38 nm (measured by ellipsometry and profilometry).

Polymer Synthesis. 20% (w/v) monomer solutions containing either PEGMA (Aldrich, MW 475) or glycidyl methacrylate (GMA, Aldrich) in dioxane (BDH Chemicals, UK) were chromatographed through a glass column filled with inhibitor remover (Aldrich). The monomer solutions were then combined in PEGMA/GMA ratios of 1:1, 2:1, and 1:2 (v/v). The thermal initiator 2,2′-azobisisobutyronitrile (AIBN, Aldrich) was then dissolved in the PEGMA/GMA solutions at a ratio of 1 mg of AIBN to 2 mL of monomer solution. The solutions were purged with nitrogen for 15 min and then sealed and placed into a 60 °C oven overnight. The solutions were then used in subsequent experiments after cooling to room temperature.

Spin Coating. A freshly prepared 20% (w/v) PEGMA/GMA copolymer solution with a PEGMA/GMA ratio of 1:1 was diluted with dioxane to a 2.5% (w/v) solution and 0.2% (w/v) 0,0′-bis(2-aminoethyl)polyethylene glycol (PEG diamine, MW = 3400, Fluka, Germany) was added and dissolved to act as a cross-linker. Freshly prepared ALAPP-coated glass slides were then placed on the spin coater (Laurell Technologies Corporation WS-400B-6NPP/Lite, USA) and covered with the solution containing the cross-linker using a glass pipet. The substrates were then spin-coated at 5000 rpm for 30 s. The resulting films were stored overnight in a vacuum chamber in order to remove the remaining dioxane and to allow for cross-linking to occur. The slides were then removed from the vacuum chamber, washed in PBS buffer (pH 7.4) at 37 °C for 2 h, washed with Milli-Q water, and dried in a spin dryer before printing.

Dip Coating. Freshly ALAPP-coated glass slides were incubated in 20% (w/v) PEGMA/GMA copolymer solutions (1:1, 2:1, and 1:2 ratios) in dioxane at room temperature overnight. Slides were then washed for 5 h in dioxane and dried in a laminar flow cabinet. In addition, slides were washed in phosphate-buffered saline (PBS) buffer (pH 7.4) at 37 °C for 2 h, washed with Milli-Q water and dried in a spin dryer before printing.

Grafting. Freshly ALAPP-coated glass slides were placed into a 20% (w/v) solution containing both PEGMA and GMA monomers (1:1 w/w ratio) and the thermal initiator AIBN was added (ratio of 1 mg of AIBN to 2 mL of monomer solution) under nitrogen. Polymerization was carried out in an oven at 60 °C overnight. The samples were then removed from the polymerization solution and washed extensively in dioxane, followed by drying in a laminar flow cabinet. Slides were then incubated in PBS buffer (pH 7.4) at 37 °C for 2 h, washed with Milli-Q water and dried in a laminar flow cabinet before printing.

All methods employed here to prepare polymer coatings with different compositions and the codes used throughout this study are shown in Table 1.

XPS Analysis. X-ray photoelectron spectroscopy (XPS) analysis of surface modified samples was performed on an AXIS HSi spectrometer (Kratos Analytical Ltd., UK), equipped with a monochromatised Al Kα source. The pressure during analysis was typically 5×10^{-8} mbar. The elemental composition of samples was obtained from survey spectra, collected at a pass energy of 320 eV. Binding energies were referenced to the aliphatic carbon peak at 285.0 eV. High-resolution elemental spectra were recorded at a pass energy of 40 eV.

Ellipsometry. As glass substrates are not suitable for ellipsometric analysis because of their transparency, silicon wafers were surface-treated according to the same procedures as described above. Measurements[33] were performed using an SE 400 (SENTECH Instruments GmbH, Germany) on the surface of the sample at multiple angles of 40, 45, 50, 55, and 60° at room temperature, considering the refractive index of silicon and silicon dioxide as 3.85 and 1.46, respectively. The ellipsometer was equipped with a helium/neon laser of a wavelength of 632.8 nm. A minimum of 10 measurements were carried out on each sample. Thickness measurements were also performed on coatings that had been soaked for 2 h in PBS at 37 °C, washed with Milli-Q water and dried under a stream of nitrogen gas.

Profilometry. A profilometer (DEKTAK 6 M Stylus Profilometer, Veeco, USA) was used to measure the thickness of the polymer layer on the glass slides. Coated slides were scratched using a metal needle and placed under the profilometer. A section analysis of the scratch was then performed, giving the height difference between the glass surface and the surface of the coating.

Fourier Transform Infrared Spectroscopy. Fourier transform infrared measurements were carried out using a Nicolet Avatar 370 MCT (Thermo, Australia) and a diffuse reflectance accessory supplied with the instrument. A total of 60 scans were averaged with a spectral resolution of 4 cm^{-1}. The sample compartment was purged with dried air (Parker-Hannifin Corporation, USA).

Microarray Printing. Fluorescein isothiocyanate-labeled bovine serum albumin (BSA-FITC; Sigma) was used as a model biomolecule for microarray printing. Stock solutions of BSA-FITC with 1 mg/mlL concentration were separately prepared in solutions of pH 5, 7, 9 and 10 in a dark vessel. Further dilution of the stock solution was performed in the respective pH solutions to yield protein solutions with concentrations of 50, 75, 100, and 200 μg/mL. All solutions were refrigerated until further use.

For cell attachment studies, different biological factors and synthetic polymers (all obtained from Aldrich) were microarrayed. Solutions were prepared in six concentrations (12.5, 25, 50, 100, 150, and 200 μg/mL) by diluting from a stock solution of 1 mg/mL concentration. Stock solutions of wheat germ agglutinin (WGA), concanavalin A (CONA), peanut agglutinin (PNA), BSA, fibronectin from bovine plasma (FBR), and laminin (LMN) were prepared in PBS (pH 7.4) cooled to 4 °C. Solutions of collagen type I (Coll I) and collagen type IV (Coll IV) were prepared in 0.1 M acetic acid cooled to 4 °C. Solutions of amine-terminated polyamidoamine (PAMAM) dendrimer, poly(ethylene imine) (PEI), and polyallylamine (PAA) were prepared in Milli-Q water cooled to 4 °C. All solutions were stored at −18 °C until further use. After thawing the frozen solutions with the help of a minishaker (IKA, Germany), 20 μL of each solution was pipetted into a 384-well source plate, which was placed on ice. The solutions were pipetted to the different wells of the source plate according to the microarray layout designed for each experiment. The source plate was immediately placed into a BioOdyssey Calligrapher (Bio-Rad, Australia) contact microarrayer after transfer of the solutions. The following printing conditions were used: Pin approach speed to the source plate and glass slide was 15 and 5 mm/s, respectively; dwell time in source plate and on glass slide were 1000 and 35 ms, respectively. Three different pins were used: A round solid pin (SSP015, ArrayIt, USA) with a tip diameter of 375 μm, a square solid pin (SNS10, ArrayIt) with a tip diameter of 335 μm and a quill pin (SMP10, ArrayIt) with a tip diameter of 335 μm. Printing was performed by varying different parameters such as pH, temperature, humidity, protein concentration, and type of pins. Glass slides were stored at 4 °C for 10 h after printing and were subsequently washed and soaked in 37 °C PBS for 2 h, then washed with Milli-Q water and dried using dry nitrogen gas. The analysis of printed glass substrates was carried out using an GenePix 4000A (Molecular Devices, USA) microarray scanner at a resolution of 10 μm.

Cell Culture. Protein microarrays were transferred to four-well tissue culture polystyrene (TCPS) trays (Nunc Multidish, Thermo Fisher Scientific, Roskilde, Denmark), and rehydrated overnight at 37 °C with a solution of PBS buffer (pH 7.4) containing penicillin and streptomycin (both from CSL) at concentrations of 120 and 200 μg/mL, respectively. HeLa cells were then seeded at 1.0×10^6 cells/well and incubated for a further 24 h in Dulbecco's modified Eagle's medium (DMEM)/Ham's F12 culture medium (MP Biomedicals, Australia) containing 10% (v/v) fetal bovine serum (FBS; P.A. Biologicals, Australia). The cells were then labeled with CellTracker Orange (CTO, Invitrogen, Australia) for the final hour of incubation, washed with PBS and then fixed with 4% formol-saline. For qualitative analysis of cell attachment, areas of the samples or individual spots were viewed by fluorescence microscopy (Nikon Eclipse 90i, Nikon, Japan) with either 2× or 10× objectives using an excitation wavelength of 540 nm. Digital images were acquired from selected areas. Quantitative analysis of cell attachment was carried out by first scanning each array slide on a Molecular Dynamics Typhoon 8600 Phosphor Imager (GE Healthcare, Australia), set at a resolution of 50 μm and an excitation wavelength of 526 nm. Quantitative information was then extracted from the resultant scanned image via the Array Analysis module in ImageQuant TL software (GE Healthcare) to generate relative fluorescence intensities for each microarray spot. The resulting fluorescence volume for each scanned spot was a function of the mean signal intensity generated by the CTO-labeled cells attached to the spot and the defined object area that was kept constant for each spot. The resultant fluorescence intensities could then be expressed as either a percentage of a nominated control value, or as an absolute fluorescence volume value.

Results and Discussion

In the present study, we aimed at generating multifunctional surface chemistries with excellent substrate adhesion that enable the covalent immobilization of biomolecules in a printed microarray format while at the same time providing a low cell attachment background between printed spots. In order to achieve this aim, we synthesized random copolymers of PEGMA and GMA with the goal to coat microarray slides with these polymers. An allyl amine plasma polymer layer was used to allow the covalent anchoring of a subsequently deposited copolymer layer on the one hand and to achieve excellent adhesion on a variety of substrate materials on the other. The GMA component provides reactive epoxy groups, enabling covalent anchorage of the coating to the amine plasma polymer layer and, at the same time, biomolecule immobilization,[34] while the PEGMA component provides the low background cell attachment between printed spots.[35] This effect is attributed to the well-known low protein fouling properties of PEG-based coatings.[36] The coating strategy used and the monomers used here are schematically shown in Figure 1. The figure illustrates the presence of the two components provided by the copolymer, the PEG chains, and the epoxy groups from the PEGMA and GMA monomers, respectively. Furthermore, the figure illustrates the covalent attachment of an amino-functional biomolecule within a printed spot on a microarray through the reaction with an epoxy group[34] as well as the fate of epoxy groups that are not used for the immobilization of biomolecules. These epoxy groups form vicinal diols upon extended exposure to an aqueous solution.[37]

Figure 2 schematically describes the different routes that were used in this study for the modification of substrate surfaces.

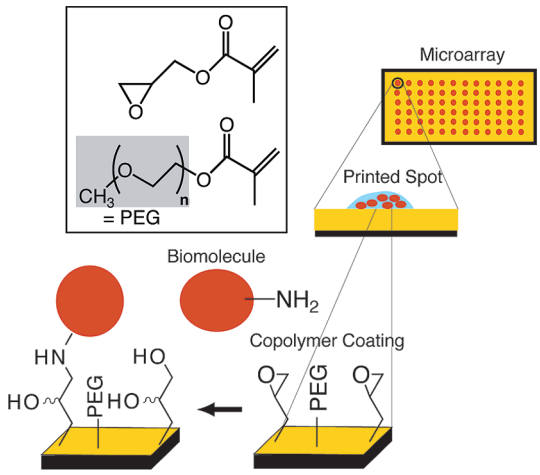

Figure 1. Schematic representation of the surface chemistry used for the surface immobilization of various biological factors on multifunctional copolymer coatings. The box shows the structure of the two monomers used here, GMA and PEGMA.

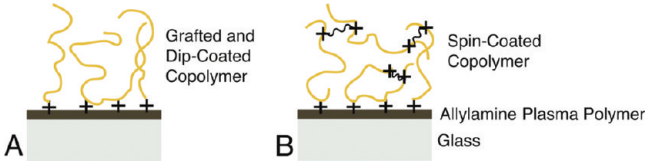

Figure 2. Multifunctional copolymer coating techniques used for the preparation of microarray substrates. Immobilization of PEGMA/GMA polymer chains on the ALAPP plasma polymer surface and cross-linking with PEG diamines (black wavy lines) is illustrated via the "+".

Dip coating, graft polymerization, and spin coating of PEGMA/GMA copolymers was carried out on glass slides and silicon wafers. The different coating methods were compared in terms of surface chemistry and protein reactivity. All three methods used an ALAPP as the base coating. The use of a highly cross-linked ALAPP layer provides excellent substrate adhesion, introduces amino functional groups[27] for subsequent reaction with the epoxy groups in the PEGMA/GMA copolymers, and allows the straightforward transfer of the coating method between different substrate materials. In the dip coating (DC) and spin coating (SC) approach, immobilization of PEGMA/GMA polymer chains occurred on the plasma polymer surface via one or more covalent attachment points schematically shown as a "+" in Figure 2. In the case of the spin coating approach, a PEG diamine was added to the spin coating solution to afford cross-linking of the spin-coated film in addition to the covalent surface attachment of the copolymer as shown in Figure 2B. The grafting (G) approach, in which PEGMA and GMA monomers are copolymerized in the presence of an ALAPP-coated substrate, also leads to the scenario seen in Figure 2A where PEGMA/GMA copolymers formed in solution were covalently immobilized on the ALAPP surface via reaction of an epoxide on the growing polymer with an amine displayed on the surface.

Table 1 shows a list of the different copolymers used in this study. Three different copolymer ratios (2:1, 1:1, and 1:2 (w/w)) were synthesized for the dip coating method, while a ratio of 1:1 (w/w) was used for both the grafting and the spin coating method.

To enable ellipsometry-based characterization of the coating thickness obtained by these different methods, we deposited the coatings onto ALAPP-coated silicon wafers. In addition, profilometry measurements were carried out on both silicon and glass substrates. The thickness of the ALAPP pinning layer was measured to be approximately 38 nm by profilometry, which is in close agreement with the value of 42 ± 0.6 nm measured by ellipsometry. An average thickness of 73 ± 7.1 nm was obtained for DC1:1, whereas a thickness of 72 ± 2.4 nm and 62 ± 10.0 nm was determined for SC1:1 and G1:1, respectively. These values measured by ellipsometry are the sum of ALAPP and PEGMA/GMA copolymer thickness and were measured after washing of the samples for 2 h in PBS at 37 °C to remove loosely bound polymer. The values were also in good agreement with profilometry measurements performed on glass substrates. A significantly smaller standard deviation in the ellipsometric thickness was observed for spin-coated samples compared to samples that were dip-coated or grafted, which indicated that only the spin coating method allowed the deposition of a polymer coating of uniform thickness.

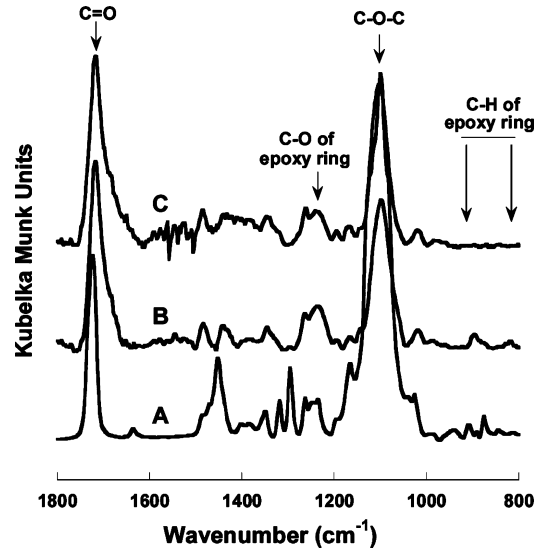

Figure 3. Diffuse reflectance infrared spectra of spin-coated copolymer SC1:1, coated on an ALAPP-coated silicon wafer substrate. Spectra were obtained after (A) coating of the copolymer, (B) incubation for 2 h in PBS at 37 °C, and (C) incubation for 24 h in PBS at 37 °C.

While it is essential to remove loosely bound polymer from the polymer-coated surfaces, the exposure to aqueous buffer for 2 h could potentially result in the quenching of the epoxy functional polymer, preventing the desired covalent immobilization of printed biological factors. We therefore carried out IR analysis in diffuse reflectance mode to investigate whether the soaking in PBS affects the oxirane rings of the GMA component of a spin-coated sample. Here, silicon was used as the substrate surface. Diffuse reflectance infrared spectra for a 1:1 PEGMA/GMA copolymer coating prepared by spin coating on an ALAPP−silicon surface before and after incubation in PBS are presented in Figure 3. Spectrum A was collected for a freshly spin-coated copolymer (SC1:1) after cross-linking overnight. In this spectrum, the peak at 1240 cm^{-1} was attributed to the symmetrical expansion and contraction vibration of the C−O of the oxirane ring, while the peak at 1020 cm^{-1} was assigned to the C−O−C ether linkage. Likewise, the peaks at 950−810 cm^{-1} were assigned to the deformed C−H vibrations of the oxirane ring. Finally, the characteristic peaks of the carbonyl groups of the methacrylate esters appeared at 1720 cm^{-1}.[38] Subsequent soaking of the surface in PBS at 37 °C for 2 h (spectrum B), results in an attenuation of the characteristic peaks of the oxirane rings at 950−810 cm^{-1}. However, the spectrum

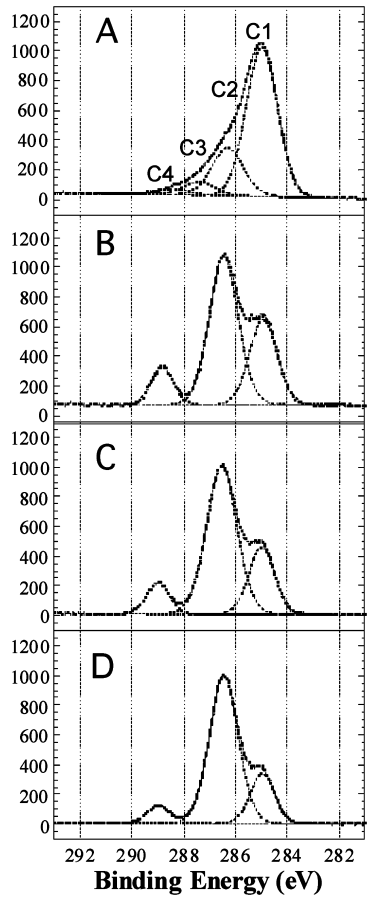

Figure 4. XPS high-resolution C1s spectra collected on surface-modified glass substrates. The spectra represent ALAPP-coated glass (A), DC1:1 (B), G1:1 (C), and SC1:1 (D) surfaces.

shows that epoxy groups remain on the coating, available for nucleophilic attack by protein molecules. After soaking for 24 h (spectrum C), however, these signals have all but disappeared, providing evidence for the effective quenching of the epoxy groups. Hence the surfaces were soaked in PBS only for 2 h prior to microarray experiment in order to remove the unbound polymer chains from the surfaces. Overnight soaking of the surfaces in PBS was applied after microarray printing to quench the epoxy groups and prevent the reaction with factors present in the cell culture medium.

XPS was used as an analytical tool to investigate the surface chemistry of the coatings. Table S1 (Supporting Information) shows the elemental composition obtained from survey spectra for the ALAPP surface, as well as for DC1:1, G1:1, and SC1:1 samples. The complete attenuation of the Si signal from the underlying glass substrate found for all of these samples confirms that the deposition of the ALAPP film created a stable, pinhole-free coating with a thickness of more than 10 nm (the approximate information depth of the XPS method). ALAPP coatings have previously been shown to provide amino functional groups.[30,39] This is indicated here by the significant increase in the nitrogen content (Table S1) and the high resolution C1s and N1s spectral information (vide infra). In comparison, none of the PEGMA/GMA coatings (DC1:1, G1:1, and SC1:1 samples) showed significant amounts of nitrogen, confirming the ellipsometry results that, in each case, a coating thickness of at least 10 nm was achieved. Figure 4 shows the XPS C1s high-resolution spectra recorded on the ALAPP-coated glass surface (A), on DC1:1 (B), G1:1 (C), and SC1:1 (D) surfaces. In addition, Table S2 shows the quantification of the components C1−C4 fitted to these spectra, with component C1 (at 285.0 eV) representing the aliphatic hydrocarbon peak (C−C/C−H), C2 representing C−O- and C−N-containing functional groups, C3 representing C═O- and N−C═O-containing functional groups, and C4 representing O−C═O-containing functional groups.

The C 1s spectrum of the ALAPP coating seen in Figure 4A shows the typical profile of a plasma polymer with a broad peak due to the variety of functional groups present. Here, the intensity of the C2 peak associated with C−O- and C−N-containing groups provides further support that ALAPP films retain a high degree of the amine functionality. In comparison, the components C3 and C4 show a much lower intensity. Compared to the ALAPP spectrum, the high-resolution C 1s spectra of the different PEGMA/GMA-coated surfaces (Figure 4B−D) are similar and show the expected dominant C2 peak due to the presence of the covalently attached graft copolymer containing ether and epoxy groups. The presence of the ester group, which is present both in PEGMA and GMA, is confirmed by component C4. The particularly high C2/C ratio for the spin-coated sample may be explained by the presence of PEG cross-linker in this coating. In summary, all surface characterization methods confirmed that the three coating methods used in this study resulted in the formation of stable polymer coatings with a sufficient thickness while displaying epoxy groups through the GMA component for the subsequent attachment of biomolecules and providing PEG chains through the PEGMA component for a low cell attachment background.

In order to optimize printing parameters on the multifunctional coatings described above, we first used a fluorescent model protein, BSA-FITC. In all cases, printing was performed on slides washed in PBS at 37 °C for 2 h to remove loosely bound polymer. Scanning of the printed slides was then performed after soaking the slides overnight in PBS (pH 7.4), washing in Milli-Q water, and drying under a stream of nitrogen gas.

Temperature and humidity are known to play an important role in the immobilization of proteins on surfaces. The temperature at which the slide is held determines the kinetics of protein immobilization, while the humidity influences the rate of evaporation of the nanoliter droplets of protein solution. Therefore, initial experiments were performed to study the effect of temperature in the range of 5−15 °C. Here, BSA-FITC was printed on a DC1:1 slide at a relative humidity (RH) of 65% using a protein concentration of 75 μg/mL, prepared in a pH 5 buffer. Higher deposition temperatures than 15 °C were not used, as this resulted in rapid evaporation of the printed solution. Pilot experiments showed that such rapid evaporation is unfavorable and leads to poorly reproducible printed protein spots. The images of the slide printed at different temperatures are represented in Figure 5A, where (I), (II) and (III) represent spots printed at 5, 10, and 15 °C, respectively. It is apparent from the images that 10 and 15 °C are better suited for the printing of the protein on the reactive substrates, whereas spots are incomplete when printing was performed at 5 °C, possibly because of the low reactivity at that temperature. As a result, we selected 10 °C for subsequent experiments in order to slow down the evaporation of solvent from printed protein solution, allowing the immobilization reaction from the liquid phase to proceed for a longer time.

We next examined the influence of humidity. Figure 5B shows the effect of humidity on protein attachment on a DC1:1 slide printed at 10 °C. Figure 5B I−IV shows images where printing was performed at 34, 45, 55, and 65% RH, respectively. The spots are not circular and almost washed off in the case of

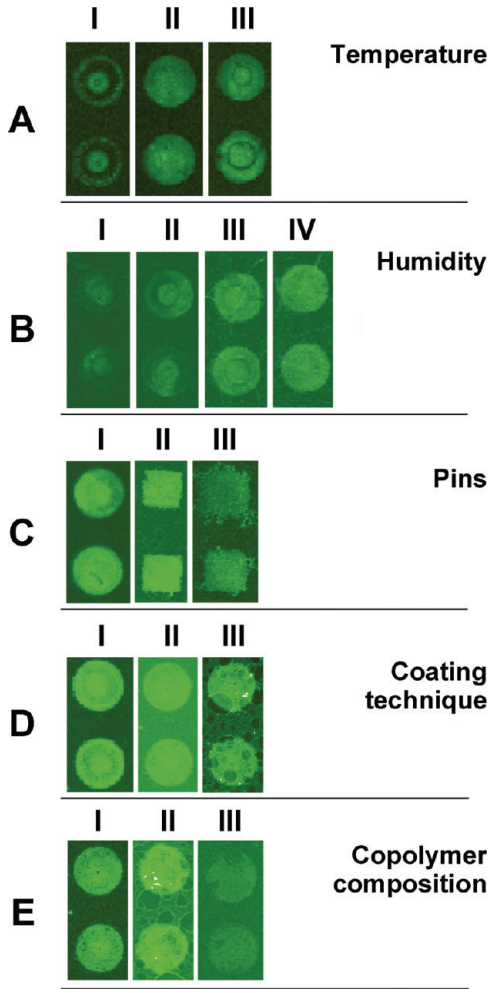

Figure 5. Fluorescence scans of BSA-FITC printed on (A) DC1:1 with a protein concentration of 75 μg/mL at pH 5 at (I) 5 °C (II) 10 °C and (III) 15 °C; (B) DC1:1 at different RHs of (I) 35%, (II) 45%, (III) 55%, and (IV) 65%; (C) SC1:1 using (I) solid round pins, (II) solid square pins, and (III) quill square pins; (D) slides representing different coating methods with (I) SC1:1, (II) DC1:1, and (III) G1:1; and (E) slides representing different copolymer compositions of (I) DC1:1, (II) DC2:1, and (III) DC1:2.

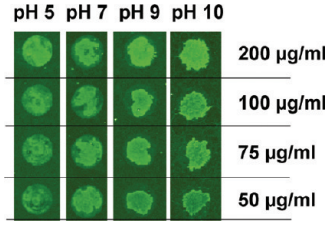

Figure 6. Fluorescence scans of arrays of BSA-FITC printed onto SC1:1 coated glass slides using different protein concentrations and buffer pH.

spots printed at 35, 45, and 55% RH. This may be due to the fast evaporation of solvent from printed protein solution printed at lower humidity conditions. However, spots printed at 65% RH remained attached to the surface. Therefore, 65% RH was used in further experiments.

BSA-FITC was printed on the SC1:1 substrate using different microarray pins including round solid, square solid and quill pins with a diameter of 375, 335, and 335 μm, respectively, to determine the final spot geometry and their stability after overnight PBS soaking. Scans of the resulting protein arrays printed with round solid, square solid, and quill pins are shown

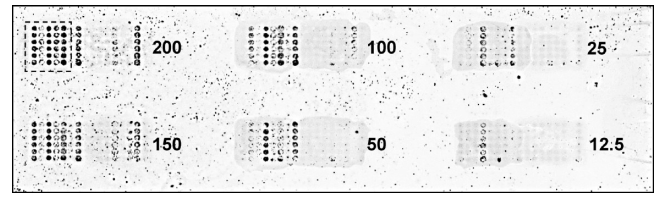

Figure 7. Shows the primary scanned microarray as captured by the Phosphor Imager. CTO-stained HeLa cell attachment to various factors after 24 h incubation is indicated by the relative amount of fluorescence signal on each array spot. Factors were printed in columns of six replicates. The number beside each block in the array indicates the spotting solution concentration (200, 150, 100, 50, 25, and 12.5 μg/mL).

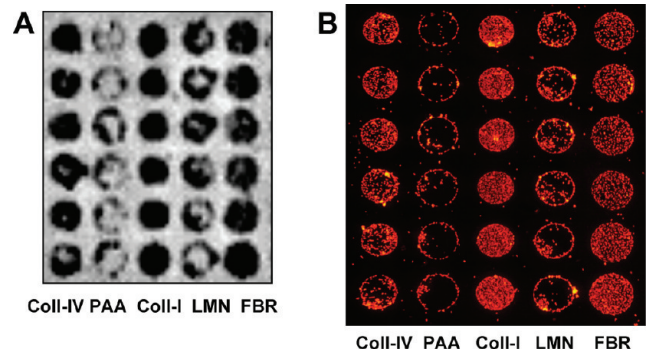

Figure 8. (A) Magnified image of part of the 200 μg/mL array set in the dashed square in Figure 7. (B) Fluorescence microscopy image (original magnification 2×) of the region shown in (A). The respective factors used here are listed beneath each array column.

in Figure 5C I−III. The images demonstrate that both round and square solid pins gave good protein distribution within the spots. Solid round pins gave the most consistent geometrical shape and morphology and were therefore used in further experiments. In contrast, spots fabricated using the quill pins were as homogeneous in size and morphology. Furthermore, since there are issues in terms of reproducibility, clogging, and cross-contamination associated with the use of quill pins,[40] we decided to use solid pins in the subsequent experiments.

Figure 5D shows protein spots printed onto (I) SC1:1, (II) DC1:1, and (III) G1:1 samples in order to compare the different coating methods in regard to protein attachment. The figure demonstrates that circular spots with a uniform protein distribution were obtained in the case of SC1:1 and DC1:1. In comparison, the G1:1 coating resulted in a nonuniform protein distribution. The result seen in Figure 5D III may be due to an uneven coating morphology. The information provided by Figure 5D suggests that the spin coating and dip coating methods yield more uniform and reliable surface coatings for the immobilization of biomolecules in a microarray format.

Figure 5E finally shows protein spots printed onto (I) DC1:1, (II) DC2:1, and (III) DC1:2 coatings to confirm that the PEGMA/GMA 1:1 (w/w) monomer ratio determined in preliminary experiments was indeed suitable for optimal attachment of printed proteins under the chosen conditions. The fluorescence scans clearly show that circular protein spots with a uniform distribution were obtained on the DC1:1 surface. In comparison, the DC2:1 surface gave nonuniform protein spots, which may be explained by an uneven coating produced at this monomer ratio. In the case of DC1:2 (higher content of reactive epoxy groups), the protein spots are less clearly visible compared to the background coating, which may point to protein binding between printed spots during washing or alternatively to cross-linking of reactive groups before protein printing. We have not

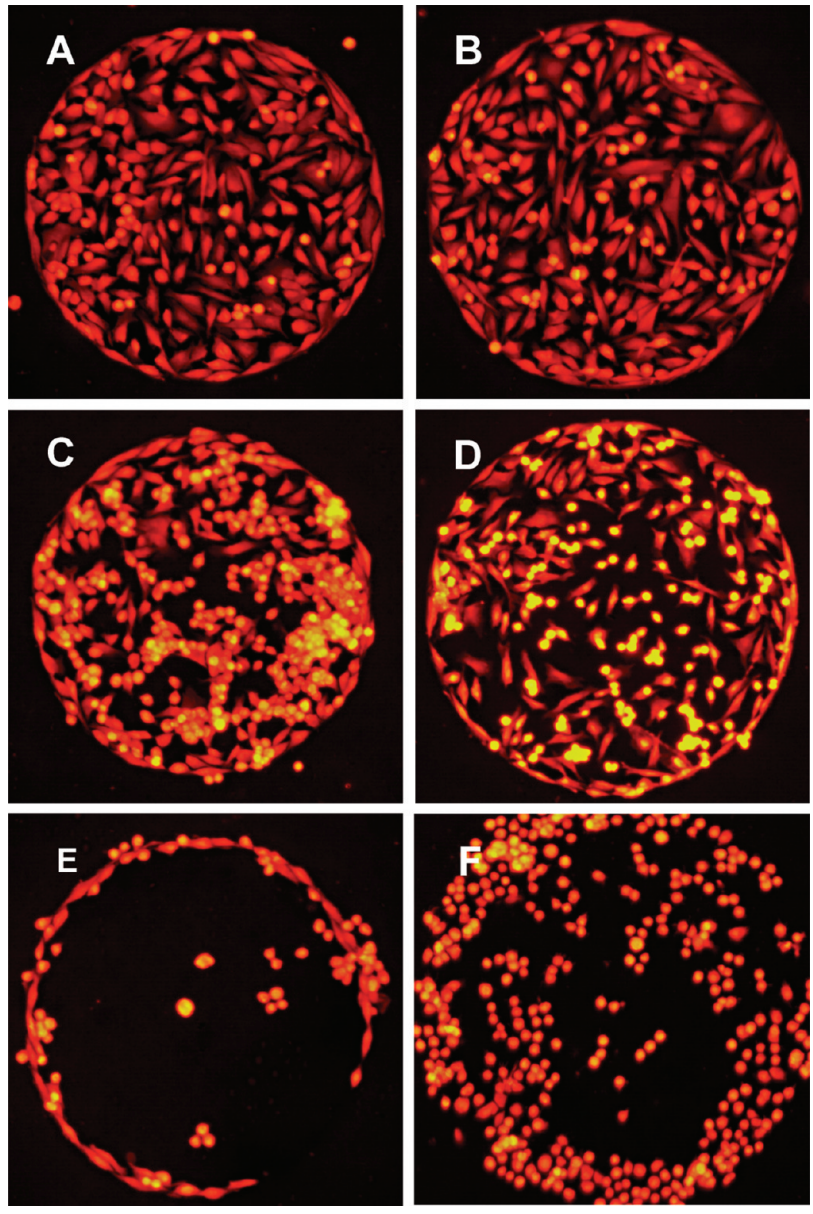

Figure 9. Representative fluorescence microscopy images of HeLa cells attached to individual array spots printed using various concentrations of Coll-I (A−E) after 24 h incubation in serum containing culture medium (original magnification 10×). The images represent concentrations of (A) 200 μg/mL, (B) 150 μg/mL, (C) 100 μg/mL, (D) 50 μg/mL, and (E) 12.5 μg/mL. (F) shows HeLa cells attached to a PAMAM spot printed at a concentration of 200 μg/mL.

investigated this issue further, since the results show that 1:1 PEGMA/GMA coatings were indeed best suited for our microarray studies.

Overall, the results obtained from surface analysis and the screening of different printing conditions suggested that spin-coated slides with a SC1:1 coating were best suited for microarray applications, providing an even, reproducible thickness and an excellent substrate for the printing and immobilization of proteins and other biomolecules. SC1:1-coated slides were therefore used in all subsequent experiments. Furthermore, solid round pins with a diameter of 375 μm were used in all subsequent experiments, and printing was always carried out at a temperature of 10 °C and a RH of 65%.

To determine the optimum protein concentration and pH at which uniform circular spots were reproducibly obtained, four protein concentrations (200, 100, 75, and 50 μg/ml), printed at four different pH conditions (5, 7, 9, and 10) were used on SC1:1 slides at 10 °C and 65% RH. Images obtained on these slides are reproduced in Figure 6. Printing at all four protein concentrations resulted in clearly visible spots with sufficient fluorescence intensities and signal-to-noise ratios. When printing was performed at pH 5 and 7, spots were circular, while spots printed at pH 9 and pH 10 had irregular outlines. On the other hand, spots printed at pH 9 and 10 appeared to result in better signal-to-noise ratios. Since most of the biomolecules and synthetic polymers used in this study were soluble at neutral pH, the printing of factors for subsequent cell microarray investigations was preferably performed from protein solutions at pH 7.4.

With the above empirically optimized conditions, various factors were microarrayed on SC1:1 slides with a center-to-center spot distance of 600 μm. We chose a range of biological factors (extracellular matrix proteins and lectins) as well as synthetic macromolecules (positively charged branched and linear polymers), with potential cell membrane activity via either specific ligand−receptor recognition or electrostatic effects. Six

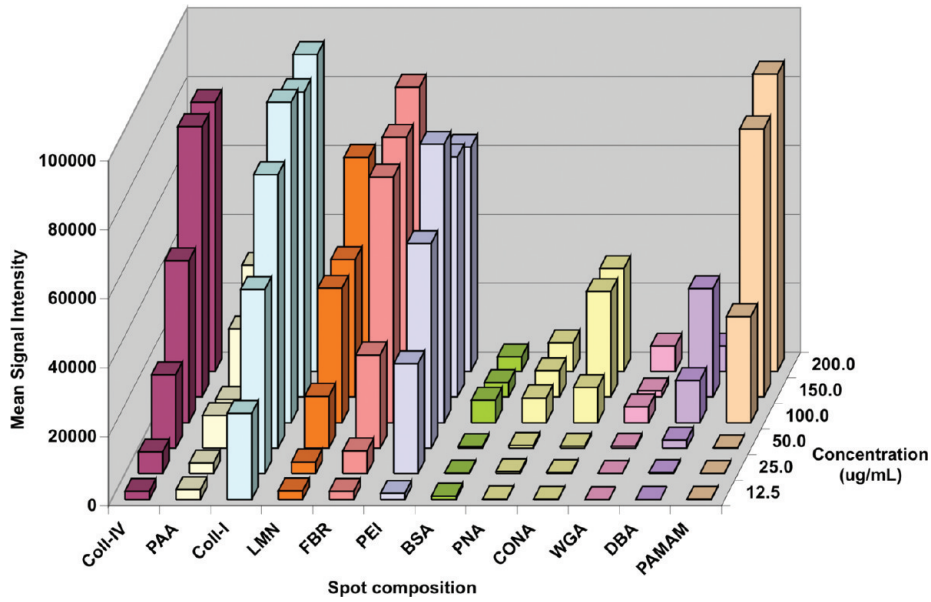

Figure 10. Relative quantitative HeLa cell attachment to various factors after 24 h of incubation in the presence of serum-containing culture medium. The data were derived from a Phosphor Imager scan, and the histogram is based on mean array data from six replicate spots per concentration for each factor.

different grids were microarrayed representing six different concentrations of factors and six replicates (in vertical columns) for each factor and concentration (Figure 7). Each printed slide was controlled in regard to printing quality and completeness using a magnifying glass. After completing the printing process, slides were kept at 4 °C overnight before cell seeding experiments.

When the development of any cell-based array system is undertaken, it is important to be aware of the need to provide a base substrate that reduces background cell attachment while simultaneously delivering a sufficiently reactive surface that maximizes the location and retention of printed factors that are to be tested. While this arrangement should subsequently allow for the accurate and reproducible capture of quantitative data on the individual cells attached to a particular spot on the array, the system's high throughput capability is predicated on access to high-speed capture of spot-level information. This second capability clearly benefits from the reduced contribution of signal from the background and the visualization of clearly identifiable array spots containing the cell-based information.

HeLa cells were chosen for this study since they provide a well-characterized cell line that maintains a consistency of response to a given surface. This characteristic allowed for a greater degree of confidence in the measurement of cellular responses to changes in array spot composition. HeLa cells were seeded onto a variety of different attachment factors that had been deposited at several different concentrations in a defined array on a low cell attachment background substrate as described above. The cells were incubated on the array for 24 h and labeled with a fluorescent dye that could be measured when scanned with a Phosphor Imager to obtain relative quantitative information. Following scanning, these same arrays were then inspected microscopically to obtain higher resolution images of individual spots, affording cell-level information. Figure 7 shows a representative scanned array on which fluorescently labeled cells have attached to six replicate array spots representing different signals (columns) at six different concentrations (as shown in the figure). Cell attachment to printed spots was clearly differentiated from the background substrate, where far fewer cells could be detected; the low background cell distribution was also notable for its random nature, unlike the tightly defined cell adherence to the array spots. Moreover, a range of spot fluorescence intensities corresponding to different cell densities are evident. Figure 8A shows a magnified view of the dashed square in Figure 7 corresponding to a subset of five printed factors, and Figure 8B shows the same region imaged with a fluorescence microscope. In Figure 8B, individual cells can be distinguished and counted, in this case showing a wide range of cell densities from less than 50 cells per spot for PAA to more than 400 cells per spot for Coll-I. Also of note is the low spot-to-spot variability among the six replicates. Comparison between Figure 8A and 8B demonstrates excellent qualitative agreement between spot fluorescence intensity and cell density. Figure 9 shows representative micrographs of HeLa cells attached to individual array spots of Coll-I printed at different concentrations (200−12.5 μg/mL). The images show a high cell density with a well-spread morphology for the higher concentrations, whereas sparsely populated array spots containing a higher proportion of rounded cells is seen for the lower protein concentrations. The sensitivity of the system is clearly demonstrated here since the HeLa cell response effectively mirrors what would be expected from exposure to a Coll-I concentration gradient on what is otherwise a low cell attachment surface. Figure 9F shows a representative spot for PAMAM dendrimer at a printed concentration of 200 μg/mL. Here, cell density and corresponding fluorescence intensity is very similar to the spot in Figure 9D, yet all cells on the spot show a rounded morphology. This outcome indicates that, while a particular substrate (PAMAM in this instance) can provide support for cell attachment, there is little support for cell spreading. These images illustrate the need for and the quality of higher resolution morphological information that can be obtained from the arrays and that quantitative data alone should not be relied upon to provide sufficient information about cell responses to various substrata.

The high signal-to-noise ratio provided by the extremely low binding base substrate used in this study emphasizes the utility of the system and allows for the ready detection and measurement of individual array spots. This clear definition of the individual spots facilitated the accurate positioning of a customized array template created in the image analysis software of the Phosphor Imager and resulted in the generation of a fluorescent signal intensity profile for each replicate spot. These data were subsequently converted into a 3D

column plot (Figure 10), where the relative performance of the different attachment factors (averaged over the six replicates) could then be compared along with the corresponding changes in spotting concentrations within each factor series. Standard deviations about the means were not included in this plot in the interests of clarity; however, representative values are included in Table S3.

Often when comparing similar experimental runs in cell-based assay systems, it is convenient to include an internal control surface to allow for inter-run comparison. In this study, we nominated Coll-I at a spotting concentration of 100 μg/mL as our reference substrate and then compared the cell-based fluorescent signals from all other array spots against this standard. The results for cell attachment relative to Coll-I are shown in Table S3. The generation of data sets as seen in Table S3 allow rapid comparisons between experimental runs and the opportunity to readily combine data sets from multiple runs.

The purpose of these cell experiments was not to identify new cell−material surface interactions, but rather to demonstrate that the copolymer coatings prepared and characterized here fulfill the requirements for microarray coatings in terms of stability, reactivity toward biomolecules, reproducibility of biomolecule attachment, low cell attachment background, and finally compatibility with microarray analysis.

Conclusions

In this study, we have demonstrated the successful coating of glass slides with random copolymers of GMA and PEGMA using three different coating methods. These copolymer coatings were shown to display reactive functional groups suitable for the covalent immobilization of factors that can influence the cellular response while at the same time exhibiting low nonspecific protein adsorption and cell attachment properties. XPS and Fourier transform infrared (FTIR) experiments confirmed the presence of the copolymer on the surface of samples prepared by all three coating methods. However the spin coating method was found to be most suitable for microarray applications. Conditions for protein printing were optimized in regard to printing temperature, humidity, pin geometry, protein concentration, and pH of the printing solution using an FITC-labeled protein. Cell culture experiments using HeLa cells confirmed the suitability of the PEGMA/GMA coatings for the surface immobilization of a selection of proteins and lectins, as well as synthetic polymers, while providing a low cell attachment background at the same time. The overall behavior of the HeLa cells on the respective coatings was within the expectation of how such cells would perform. At the higher spotting concentrations, extracellular matrix-based coating molecules such as the collagens and fibronectin provided good levels of cell attachment and spreading, while the BSA-coated spots, for example, were unsurprisingly poor supporters of cell attachment at all concentration points. The successful use of the multifunctional coatings in a microarray application was also demonstrated. Because of the increasing demand for biocompatible coatings that can be used for the display of biologically active compounds on a background displaying low nonspecific interactions, it is expected that the multifunctional coatings described in this study will find a range of biomedical applications, for example supporting dynamic new technology platforms such as cell microarray-based screening studies.

Acknowledgment. Financial support from the CSIRO Food Futures Flagship and the Flinders University's Faculty of Science and Engineering Program Grant is gratefully acknowledged.

Supporting Information Available. Tables S1 and S2 showing XPS analysis of the coatings, and Table S3 showing HeLa cell attachment to the printed factors. This material is available free of charge via the Internet at http://pubs.acs.org.

References and Notes

(1) Drickamer, K.; Taylor, M. E. *Genome Biol.* **2002**, *3*, 1034.11034.4.
(2) Huang, R. P. *J. Immunol. Methods* **2001**, *255*, 1–13.
(3) Yamazoe, H.; Iwata, H. *J. Biosci. Bioeng.* **2005**, *100*, 292–296.
(4) Castel, D.; Pitaval, A.; Debily, M.-A.; Gidrol, X. *Drug Discovery Today* **2006**, *11*, 616–622.
(5) Kononen, J.; Bubendorf, L.; Kallioniemi, A.; Barlund, M.; Schraml, P.; Leighton, S.; Torhorst, J.; Mihatsch, M. J.; Sauter, G.; Kallioniemi, O. P. *Nat. Med.* **1998**, *4*, 844–847.
(6) Grinnell, F.; Milam, M.; Srere, P. A. *Biochem. Med.* **1973**, *7*, 87–90.
(7) Angres, B. *Expert Rev. Mol. Diagn.* **2005**, *5*, 769–779.
(8) Jiang, H.-Y.; Zhang, S.-Q.; Zhao, T. *Diagn. Mol. Pathol.* **2006**, *15*, 109–114.
(9) Mikulikova, R.; Moritz, S.; Gumpenberger, T.; Olbrich, M.; Romanin, C.; Bacakova, L.; Svorcik, V.; Heitz, J. *Biomaterials* **2005**, *26*, 5572–5580.
(10) Chen, D. S.; Davis, M. K. *Curr. Opin. Chem. Biol.* **2006**, *10*, 28–34.
(11) Horlacher, T.; Seeberger, P. H. *Chem. Soc. Rev.* **2008**, *37*, 1414–1422.
(12) Ziauddin, J.; Sabatini, D. M. *Nature* **2001**, *411*, 107–110.
(13) Hook, A. L.; Thissen, H.; Voelcker, N. H. *Trends Biotechnol.* **2006**, *24*, 471–477.
(14) Anderson, D. G.; Levenberg, S.; Langer, R. *Nat. Biotechnol.* **2004**, *22*, 863–866.
(15) Anderson, D. G.; Putnam, D.; Lavik, E. B.; Mahmood, T. A.; Langer, R. *Biomaterials* **2005**, *26*, 4892–4897.
(16) Mant, A.; Tourniaire, G.; Diaz-Mochon, J. J.; Elliott, T. J.; Williams, A. P.; Bradley, M. *Biomaterials* **2006**, *27*, 5299–5306.
(17) Ito, Y.; Nogawa, M. *Biomaterials* **2003**, *24*, 3021–3026.
(18) Flaim, C. J.; Chien, S.; Bhatia, S. N. *Nat. Methods* **2005**, *2*, 119–125.
(19) Soen, Y.; Mori, A.; Palmer, T. D.; Brown, P. O. *Mol. Syst. Biol.* **2006**, *2*, 37–52.
(20) Harbers, G. M.; Gamble, L. J.; Irwin, E. F.; Castner, D. G.; Healy, K. E. *Langmuir* **2005**, *21*, 8374–8384.
(21) Grinnell, F.; Milam, M.; Srere, P. A. *Biochem. Med.* **1973**, *7*, 87–90.
(22) Bledia, Y.; Domb, A. J.; Linial, M. *Brain Res. Protoc.* **2000**, *5*, 282–289.
(23) Ouyang, E. C.; Wu, G. Y.; Wu, C. H. Biocompatible polymers in liver-targeted gene delivery systems. In *Polymeric Biomaterials*, 2nd ed.; Dumitriu, S., Ed.; Marcel Dekker: New York, 2002; p 975−981.
(24) Wu, P.; Hogrebe, P.; Grainger, D. W. *Biosens. Bioelectron.* **2006**, *21*, 1252–1263.
(25) Ramires, P. A.; Mirenghi, L.; Romano, A. R.; Palumbo, F.; Nicolardi, G. *J. Biomed. Mater. Res.* **2005**, *51*, 535–539.
(26) Lee, H. J.; Goodrich, T. T.; Corn, R. M. *Anal. Chem.* **2001**, *73*, 5525–5531.
(27) Hermanson, G. T. *Bioconjugate Techniques*; Academic Press: San Diego, 1996.
(28) MacBeath, G.; Schreiber, S. L. *Science* **2000**, *289*, 1760–1763.
(29) Kingshott, P.; Thissen, H.; Griesser, H. J. *Biomaterials* **2002**, *23*, 2043–2056.
(30) Thissen, H.; Hayes, J. P.; Kingshott, P.; Johnson, G.; Harvey, E. C.; Griesser, H. J. *Smart Mater. Struct.* **2002**, *11*, 792–799.
(31) Kannan, B.; Castelino, K.; Chen, F. F.; Majumdar, A. *Biosens. Bioelectron.* **2006**, *21*, 1960–1967.
(32) Griesser, H. J. *Vacuum* **1989**, *39*, 485–488.
(33) Losic, D.; Cole, M.; Thissen, H.; Voelcker, N. H. *Surf. Sci.* **2005**, *584*, 245–257.
(34) Mateo, C.; Fernandez-Lorente, G.; Abian, O.; Fernandez-Lafuente, R.; Guisan, J. M. *Biomacromolecules* **2000**, *1*, 739–745.
(35) Thissen, H.; Johnson, G.; McFarland, G.; Verbiest, B. C. H.; Gengenbach, T.; Voelcker, N. H. *Proc. SPIE* **2006**, *6413*, 64130B 1–9.
(36) Thissen, H.; Johnson, G.; Hartley, P. G.; Kingshott, P.; Griesser, H. J. *Biomaterials* **2006**, *27*, 35–43.

(37) Smigol, V.; Svec, F.; Frechet, J. M. J. *Macromolecules* **1993**, *26*, 5615–5620.
(38) Okubo, M.; Okada, M.; Miya, T.; Takekoh, R. *Colloid Polym. Sci.* **2001**, *279*, 807–812.
(39) Szili, E.; Thissen, H.; Hayes, J. P.; Voelcker, N. H. *Biosens. Bioelectron.* **2004**, *19*, 1395–1400.
(40) Fang, Ye; Ferrie, Y.; Fang, A. M.; Lai, F. In *The Proteomics Protocols Handbook*, 1st ed.; Walker, J., Ed.; Humana Press: New York, 2005; pp 723−732.

BM801417S